Construction of Hexagonal Basis Functions Applied in the Galerkin-Type Finite Element Method

MISAKO ISHIGURO*

A hexagonal element scheme is formulated to treat the hexagonal lattice together with the Galerkin approximation in finite element method. Presented in this paper is a method of construction of the localized Galerkin functions (shape functions) for a regular hexagon. Here, the shape functions must attain degree one approximation and provide the basis function with the property of inter-element continuity, both of which are inherent in piecewise interpolation. The hexagonal shape functions are constructed as the products of planes on four triangles constituting the hexagon. The functions thus obtained are rational fraction-type and the numerators are the lowest order polynomials within the required conditions.

1. Introduction

Treatment of a hexagonal lattice domain is often required in nuclear reactor calculations. Typical of such an example is the case of a fast breeder reactor under development for future use. Fig. 1 represents the section of a hexagonal gas-cooled fast reactor (GCFR)[1]. The section includes four fuel zones in the core, two blankets (RB) and one lateral shield zone (REFLECTOR), and control and safety rods (CRP and SRP). All the subassemblies constituting the section are identical shape, representing a regular hexagon with 12.3 cm per side.

Let n be the number of subassemblies of a section. The number of node points would be, from Fig. 2:

Hexagonal element scheme (FEM6)	$2n$
Triangular element scheme (FEM7)	$3n$
Refined triangular element scheme (FEM19)	$12n$

It is seen that the hexagonal scheme (FEM6) requires a smaller number of nodes than conventional triangular one (FEM7) for a given configuration. Therefore, using the FEM6 will bring a saving of computing time.

In the present paper, we particularly consider the application of the Galerkin method[2],[3] which is mainly used for solving the fluid flow problems. Typical of such problems found in the nuclear reactor analyses is the neutron diffusion calculation. The diffusion problem is reduced to the solution of a self-adjoint elliptic second-order partial differential equations.

The element schemes widely used in practical applications have been based on triangular or rectangular ones and a hexagon has usually been treated as six triangles. No detail study has appeared on the construction of the element scheme directly based on the hexagon. In the Galerkin method, trial functions, so called as basis functions, are particularly used as the weighting functions of a weighted residual method.

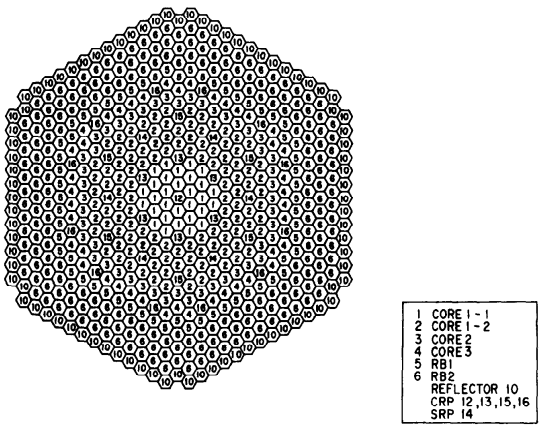

Fig. 1 Configuration of GCFR.

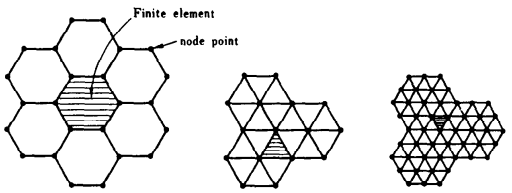

Fig. 2 Two-dimensional node point representations.

Therefore, we construct the basis function over the hexagonal lattice from a set of localized Galerkin functions (shape functions) on regular hexagon using a piecewise Lagrange-like interpolation procedure. Here, the shape functions are to be continuous across the hexagonal boundaries.

Wachspress[4] shows a method for construction of wedges which are rational fraction-type shape functions on polygons. But the shape functions in his manner violate an intuitive constraint: the sum of the shape functions has to be 1 within an element, for the convex polygons except for quadrilaterals.

*Computing Center, Tokai Research Establishment, Japan Atomic Energy Research Institute.

Another approach is possible if the domain is restricted to hexagonal lattice. We use the idea of the products of planes known as a technique applied to six point scheme on a triangle. The shape functions thus obtained are also rational fraction-type and the numerators are the lowest order polynomial under consideration.

It is too sophisticated to evaluate the convergence of finite element discrete solutions as compared with the finite difference solution. Instead of this, we shall represent the numerical results obtained from a comparison made between the above three schemes in the case of a hexagonal prism geometry. The analytical solution of similar size cylindrical geometry will be also shown.

2. Galerkin Method

2.1 Basis Functions

Dividing the domain of interest into a number of elements and numbering the node points interconnecting the elements, we obtain a discretization of the problem. The nodes are numbered on a x-y plane from 1 to N. Specifically, if $(\Omega_1, \Omega_2, \cdots, \Omega_M)$ represents a hexagonalization of the x-y plane, then each Ω_m is an element of regular hexagon constituted from the vertices 1, 2, $\cdots$, 6. For convenience, we denote vertices by the indices k and l, and node points by i and j.

Galerkin method[3] is a numerical procedure for approximating the solution of a set of differential equations of the form

$$\mathscr{L}(u)-p=0, \quad (x, y) \in V \tag{2.1}$$

with boundary conditions

$$\mathscr{S}(u)-q=0, \quad (x, y) \in S \tag{2.2}$$

where V is a domain, S is the boundary surface, x, y represent the spatial coordinates, and u is the exact solution. The function $u(x, y)$ is approximated by a set of trial functions φ_i's

$$u(x, y)=\sum_{i=1}^{N} u_i \varphi_i(x, y). \tag{2.3}$$

Galkerkin method is a particular weighted residual method in which the weighting functions are the same as the trial functions. The residual

$$\varepsilon=\mathscr{L}\left(\sum_{i=1}^{N} u_i \varphi_i\right)-p \tag{2.4}$$

is forced to be 0, in average sense:

$$\langle \varepsilon, \varphi \rangle=0, \tag{2.5}$$

which can be rewritten as

$$\int_V \{\mathscr{L}(\Sigma u \varphi)-p\}\varphi_i \, dV=0, \quad i=1, 2, \cdots, N. \tag{2.6}$$

In above, u_i represents the value of u at the i-th node $P_i(x, y)$, and the trial functions φ_i's, each associated with the node P_i, are basis functions. The problem is to find the nodal unknowns u_i's.

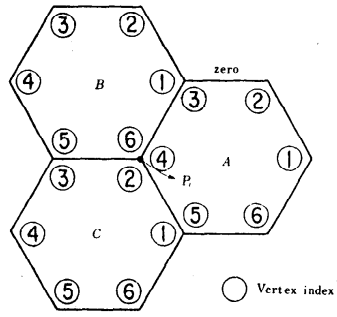

Fig. 3 Associated domain of a basis function φ_i.

Here, the basis φ_i is formed from a set of shape functions localized to the hexagonal element, and used for solving the interpolation problem[3]:

(1) $\varphi_i(P_i)=1$.

(2) $\varphi_i(P_j)=0$ for $j \neq i$.

(3) φ_i vanishes outside all elements sharing a common vertex P_i (see elements A, B, C in Fig. 3).

In addition to above three properties, the basis has to be continuous inside and between elements up to the order $n-1$, where n is the highest order derivatives in the functional[3]. The functional is a function of functions and comes from the weak formulation of the system of equations. For the harmonic equations (e.g. $\nabla^2 u=0$) this implies continuity of φ_i's and for the biharmonic equations (e.g. $\nabla^4 u=0$) it means continuity of φ_i's and $\partial \varphi_i / \partial n$'s, where n is a normal to the boundary. In particular, we concern the equations in the harmonic-type steady state problem (e.g. second-order partial differential equations) which often appears in fluid flow problems. It follows that

(4) $u(x, y)$ belongs to Sobolev space $W_2^{(1)}$. The space contains all the functions whose first derivative is square integrable. This implies that φ_i's are continuous across inter-element boundaries.

Furthermore, for most problems, it is natural to assume that all points within a hexagonal element have the same value of u as at the vertices when all six have the same value. As a consequence, the shape functions should be constructed on the constraint called a degree one approximation in Wachspress's meaning[4]: the sum of the basis functions should be 1 for all points within the element. It follows that

(5) $\sum_{i=1}^{N} \varphi_i(x, y)=1$

2.2 Piecewise Interpolation Function

Now we describe the interpolation function $\hat{u}$ to u on a hexagonal lattice.

On each hexagonal element Ω_m, we construct a function $\hat{u}(x, y)$ that interpolates $u(x, y)$ at the vertices 1, 2, $\cdots$, 6 of Ω_m. The piecewise interpolate $\hat{u}(x, y)$ is defined by

$$\hat{u}(x, y)=u_m(x, y) \quad \text{if } (x, y) \in \Omega_m. \tag{2.7}$$

The basis for computing the u_m is based on the set of

shape functions $\varphi_1, \varphi_2, \cdots, \varphi_6$ associated with the vertices 1, 2, $\cdots$, 6. It follows that

$$u_m(x, y)=\sum_{k=1}^{6} u(x_k, y_k)\varphi_k(x, y), \tag{2.8}$$

where the coordinate (x_k, y_k) corresponds to the vertex k of Ω_m.

2.3 Galerkin Application

We will show an example in the case of extended harmonic equation[3]. First deduced is a property of a single element:

$$\partial/\partial x(h\,\partial u/\partial x)+\partial/\partial y(h\,\partial u/\partial y)+\lambda u=p \quad (x, y)\in\Omega_m, \tag{2.9}$$

with boundary conditions:

$$u=\bar{u} \text{ on } S_1,\ h\,\partial u/\partial n=q \text{ on } S_2,$$

where $u=u(x, y)$, n is unit normal vector, λ is a constant, h, p, u, q are prescribed functions of x, y, and $S=S_1+S_2$ is the total boundary.

By virtue of the descriptions given in Ref. (3), the global equilibrium equation for the hexagonalization $(\Omega_1, \Omega_2, \cdots, \Omega_M)$ is rewritten as an assemblage of elements-wise matrices:

$$\begin{bmatrix} L_1 & & & & \\ & L_2 & & & \\ & & \ddots & & \\ & & & L_m & \\ & & & & \ddots \\ & & & & & L_M \end{bmatrix} \begin{bmatrix} u_1 \\ u_2 \\ \vdots \\ u_N \end{bmatrix} = \begin{bmatrix} p_1 \\ p_2 \\ \vdots \\ p_N \end{bmatrix}, \quad \text{where } L_m=K_m-\lambda M_m \tag{2.10}$$

where K_m, M_m and P_m are element matrices defined by

$$K_m=\int_{\Omega_m} h(\Phi_x^T\Phi_x+\Phi_y^T\Phi_y)\,d\Omega, \quad M_m=\int_{\Omega_m}\Phi^T\Phi\,d\Omega,$$

$$P_m=-\int_{\Omega_m} p\Phi\,d\Omega+\int_{S_1} q\Phi\,dS \tag{2.11}$$

and

$$\Phi=(\varphi_1, \varphi_2, \cdots, \varphi_N).$$

Note that K_m and M_m are symmetric matrices.

3. Hexagonal Shape Functions

3.1 Construction of Hexagonal Shape Functions

The shape functions usually used for this type of problems were planes on a triangle and bilinear Lagrange polynomials on a rectangle. Fig. 4 are the graphs of them.

We now construct the shape functions for a regular hexagon using the idea of "products of planes" which is applied for a technique to obtain the shape functions for a six-point scheme on a triangular element[5]. We also denote the shape functions by $\varphi_1, \varphi_2, \cdots, \varphi_6$.

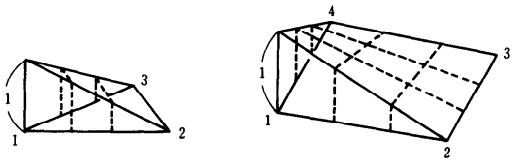

(a) Triangular element (b) Rectangular element

Fig. 4 Triangular and rectangular shape functions.

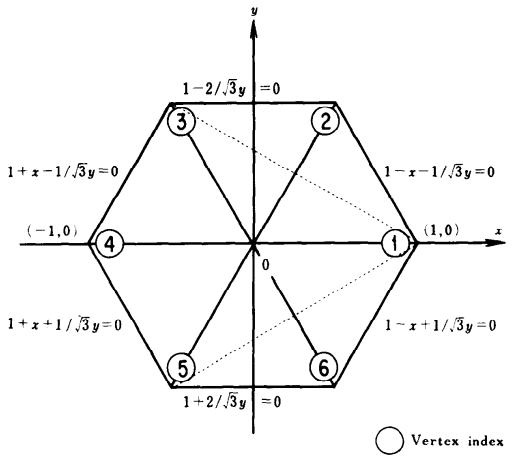

Fig. 5 Six side-line equations and partition into four triangles.

Let Ω_1 be the regular hexagon of side length 1. Computation of the φ_k's is achieved as products of planes on four triangles (see Fig. 5). On the triangle ①②③, we construct the unique plane Q_1 interpolating 1, 0 and 0 at vertices ①, ②, and ③, respectively, and on the triangle ①③④, the unique plane Q_2 interpolating 1, 0 and 0 at vertices ①, ③ and ④, respectively. The planes Q_3 and Q_4 on the triangles ①④⑤ and ①⑤⑥, are similarly formed. It is evident that

$$\varphi_1(x, y)=Q_1(x, y)Q_2(x, y)Q_3(x, y)Q_4(x, y) \tag{3.1}$$

solves the interpolation problem

$$\varphi_1(x_k, y_k)=\delta_{1k} \quad \text{for } k=1, 2, \cdots, 6.$$

In the above, Q's are given by

$$\begin{aligned} Q_1(x, y)&=\{x_2y_3-x_3y_2+x(y_2-y_3)+y(x_3-x_2)\} \\ &\quad /\{x_1(y_2-y_3)+x_2(y_3-y_1)+x_3(y_1-y_2)\} \\ &=1-2/\sqrt{3}y. \end{aligned}$$

Similarly,

$$\begin{aligned} Q_2(x, y)&=(1+x-1/\sqrt{3}y)/2, \\ Q_3(x, y)&=(1+x+1/\sqrt{3}y)/2, \\ Q_4(x, y)&=1+2/\sqrt{3}y. \end{aligned} \tag{3.2}$$

As a consequence, we obtain

$$\begin{aligned} \varphi_1(x, y)&=(1-2/\sqrt{3}y)(1+x-1/\sqrt{3}y)(1+x+1/\sqrt{3}y) \\ &\quad \times(1+2/\sqrt{3}y)/4, \end{aligned}$$

and similarly

$$\varphi_2(x, y)=(1+x-1/\sqrt{3}y)(1+x+1/\sqrt{3}y)(1+2/\sqrt{3}y)\times(1-x+1/\sqrt{3}y)/4,$$
$$\varphi_3(x, y)=(1+x+1/\sqrt{3}y)(1+2/\sqrt{3}y)(1-x+1/\sqrt{3}y)\times(1-x-1/\sqrt{3}y)/4,$$
$$\varphi_4(x, y)=(1+2/\sqrt{3}y)(1-x+1/\sqrt{3}y)(1-x-1/\sqrt{3}y)\times(1-2/\sqrt{3}y)/4,$$
$$\varphi_5(x, y)=(1-x+1/\sqrt{3}y)(1-x-1/\sqrt{3}y)(1-2/\sqrt{3}y)\times(1+x-1/\sqrt{3}y)/4,$$
$$\varphi_6(x, y)=(1-x-1/\sqrt{3}y)(1-2/\sqrt{3}y)(1+x-1/\sqrt{3}y)\times(1+x+1/\sqrt{3}y)/4. \quad (3.3)$$

Note that φ_1 is symmetrical to x-axis. The shape of φ_k's is the same, since φ_2, φ_3, φ_4, φ_5, φ_6 can be obtained from φ_1 by subsequent rotations of 60°. Next, let Ω and Ω_1 be the hexagons of side length "h" and 1, respectively. Clearly we have

$$\psi_k(x, y)=h^2\varphi_k(x/h, y/h) \quad \text{for } k=1, 2, \cdots, 6, \quad (3.4)$$

where φ_k and ψ_k denote the shape functions on Ω_1 and Ω, respectively.

The functions thus obtained have to attain the degree one approximation: $\sum_{k=1}^{6}\varphi_k(x, y)=1$, specified in Section 2.1. Whereas the sum of the functions given by Eq. (3.3) is bread shaped as pictured in Fig. 6.

Finally, after normalizing the functions (3.3) so as to force the sum to 1, we arrive at rational fraction-type functions:

$$\varphi_1(x, y)=(1-2/\sqrt{3}y)(1+x-1/\sqrt{3}y)(1+x+1/\sqrt{3}y)\times(1+2/\sqrt{3}y)/v,$$
$$\varphi_2(x, y)=(1+x-1/\sqrt{3}y)(1+x+1/\sqrt{3}y)(1+2/\sqrt{3}y)\times(1-x+1/\sqrt{3}y)/v,$$
$$\varphi_3(x, y)=(1+x+1/\sqrt{3}y)(1+2/\sqrt{3}y)(1-x+1/\sqrt{3}y)\times(1-x-1/\sqrt{3}y)/v,$$
$$\varphi_4(x, y)=(1+2/\sqrt{3}y)(1-x+1/\sqrt{3}y)(1-x-1/\sqrt{3}y)\times(1-2/\sqrt{3}y)/v,$$
$$\varphi_5(x, y)=(1-x+1/\sqrt{3}y)(1-x-1/\sqrt{3}y)(1-2/\sqrt{3}y)\times(1+x-1/\sqrt{3}y)/v,$$
$$\varphi_6(x, y)=(1-x-1/\sqrt{3}y)(1-2/\sqrt{3}y)(1+x-1/\sqrt{3}y)\times(1+x+1/\sqrt{3}y)/v,$$

where

$$v=4\sum_{k=1}^{6}\varphi_k(x, y)=2(3-x^2-y^2). \quad (3.5)$$

The function φ_1 presents the shape shown in Fig. 7, where the numbers ①~⑥ denote the vertices.

After all, the basis function $\varphi_i(x, y)$ associated with the node P_i is composed of at most three shape functions whose domain elements share a common vertex P_i (see Fig. 3 again), and $\varphi_i=0$ outside such elements. The basis thus obtained satisfies the properties (1), (2), and (3) in Section 2.1.

To validate the continuity property, we invoke the symmetry of shape function itself and the rotational symmetry between the functions. In Fig. 3, we see

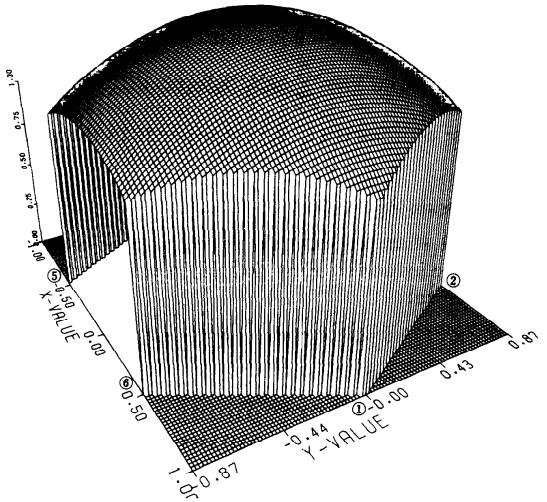

Fig. 6 Sum of six shape functions $\sum_{k=1}^{6}\varphi_k$.

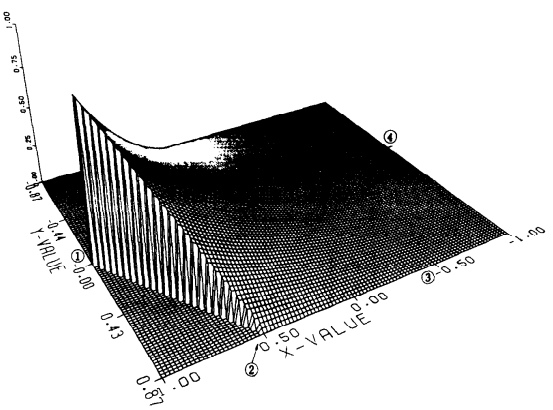

Fig. 7 Normalized hexagonal shape function φ_1.

$$\varphi_{i(4)}(x, y)^{4\overset{A}{\rightarrow}3}=\varphi_{i(6)}(x, y)^{6\overset{B}{\rightarrow}1}, \quad (3.6)$$

where, for example, $4\overset{A}{\rightarrow}3$ denotes the side from 4 to 3 on the element A and $i(k)$ is the i-th node corresponding to the k-th vertex of a hexagon. The Eq. (3.6) implies that the basis φ_i is continuous across the boundary of A and B.

In addition, from the method of construction of the shape functions given in Eq. (3.3), it is seen that the basis function φ_i vanishes along the sides opposite node i. Indeed, this feature is indispensable for the continuity property, since basis should vanish outside the associated domain and be continuous across the side lines. Obviously, the basis obtained in this manner is the lowest order polynomial under consideration in the unnormalized form.

3.2 Calculation of Integrals between Shape Functions

Now, let us consider the values related to the integral

Table 1 Value of integrals $\int \varphi_k\varphi_l d\Omega$ and $\int \varphi'_k\varphi'_l d\Omega$ for hexagonal shape functions.

Index	Shapes (3–5) by Romberg integration		Shapes (3–3) by REDUCE2	
k, l	B_{kl} ($\times h^2$)	Q_{kl}	B_{kl} ($\times\sqrt{3}/2h^2$)	Q_{kl} ($\times 2/\sqrt{3}$)
(1,1), (2,2), (3,3), (4,4), (5,5), (6,6)	0.1584735	0.7606447	9587/33600	10819/13440
(1,2), (2,3), (3,4), (4,5), (5,6), (1,6)	0.08657701	−0.1619850	7527/44800	−951/8960
(1,3), (2,4), (3,5), (4,6), (1,5), (2,6)	0.03675672	−0.1693089	10651/134400	−4477/26880
(1,4), (2,5), (3,6)	0.02787179	−0.09805682	2077/33600	−1389/13440

of shape functions over Ω. The typical ones are $\int \varphi_k\, d\Omega$, $\int \varphi'_k\, d\Omega$, $\int \varphi_k\varphi_l\, d\Omega$, $\int \varphi'_k\varphi'_l\, d\Omega$. As was seen in the expressions (2.10)~(2.11), these values are key for solving the partial differential equations by Galerkin method.

Particularly, we consider the integrals $\int \varphi_k\varphi_l\, d\Omega$ and $\int \varphi'_k\varphi'_l\, d\Omega$ which appeared in the formula for the solution of neutron diffusion equations and integrals over the hexagon of side length 1. Then we denote

$$B_{kl}=\int_{\Omega_1} \varphi_k\varphi_l\, d\Omega, \quad Q_{kl}=\int_{\Omega_1} \varphi'_k\varphi'_l\, d\Omega \quad \text{for } k, l=1, 2, \cdots, 6. \tag{3.7}$$

The above integrals are easily calculated for the triangular and rectangular schemes by a simple hand calculation[2]. But for the application of more complex shapes, the integration becomes a troublesome problems. For the polynomial-type shapes in the unnormalized form, a means for obtaining the analytical integration is to use the symbolic manipulation software REDUCE2[6] developed by the university of Utah. But for the rational fraction-type ones, it is impossible. Then, we attempt the Romberg's numerical integration with sufficient accuracy.

Let B'_{kl} and Q'_{kl} denote the integrals on the hexagon with the side length "h". Clearly we have

$$B'_{kl}=h^2B_{kl}, \quad Q'_{kl}=Q_{kl} \quad \text{for } k, l=1, 2, \cdots, 6. \tag{3.8}$$

Since the values B'_{kl} and Q'_{kl} can be easily calculated from the values B_{kl} and Q_{kl}, then these values are available for other similar problems based on a regular hexagon. Therefore, we provide the concrete values by Table 1 for both the normalized shapes in Eq. (3.5) and the unnormalized shapes in Eq. (3.3).

4. Other Methods and Discussions

As was mentioned, we first derived a set of piecewise hexagonal basis functions which were the lowest order polynomials under inter-element continuity. To make the trivial case expressible:

$$u(x, y)=\text{constant} \quad \text{where } (x, y)\in\Omega, \tag{4.1}$$

the polynomial shape functions were normalized. As a result, rational fraction-type shape functions were obtained. This constraint, however, complicates the form taken by the shape functions. Note that no linear combination of such shapes gives the interpolate u in the linear form which has been widely used in the past:

$$u(x, y)=ax+by+c \quad \text{where } (x, y)\in\Omega. \tag{4.2}$$

If the continuity property is dropped, the usual method to compute the hexagonal shape functions is to seek the quadratic surface

$$\varphi_k(x, y)=ax^2+bxy+cy^2+dx+ey+f \quad \text{for a vertex } k \tag{4.3}$$

which solves the interpolation problem on each hexagon

$$\varphi_k(x_l, y_l)=\delta_{kl} \quad l=1, 2, \cdots, 6. \tag{4.4}$$

More concretely, the unknowns a, b, c, d, e, f are to be determined from the values at the vertices $1, 2, \cdots, 6$. Especially let us consider the shape function at vertex 1, we have to solve

$$\begin{bmatrix}1\\0\\0\\0\\0\\0\end{bmatrix}=\begin{bmatrix}x_1^2 & x_1y_1 & y_1^2 & x_1 & y_1 & 1\\ x_2^2 & x_2y_2 & y_2^2 & x_2 & y_2 & 1\\ x_3^2 & x_3y_3 & y_3^2 & x_3 & y_3 & 1\\ x_4^2 & x_4y_4 & y_4^2 & x_4 & y_4 & 1\\ x_5^2 & x_5y_5 & y_5^2 & x_5 & y_5 & 1\\ x_6^2 & x_6y_6 & y_6^2 & x_6 & y_6 & 1\end{bmatrix}\begin{bmatrix}a\\b\\c\\d\\e\\f\end{bmatrix}. \tag{4.5}$$

This equation, however, is not solvable, because the resulting coefficient matrix is singular. This singularity is because the vertices are symmetrically with respect to x-axis (see Fig. 5).

Another lower-order polynomials without continuity constraint are symmetrical ones. That is, if the function φ_1 is symmetric with respect to the x-axis, then it can be written in the form

$$\varphi_1(x, y)=ax+by^2+cxy^2+d \quad \text{for a vertex } k. \tag{4.6}$$

After solving the interpolation problem at the vertices ①, ②, ③ and ④, we express it as

$$\varphi_1(x, y)=(1+x)(1-2/\sqrt{3}y)(1+2/\sqrt{3}y)/2 \quad \text{(unnormalized form)}. \tag{4.7}$$

The function φ_1, in the normalized form, is shown in Fig. 8. We see that φ_1 does not vanish on the sides ③–④ and ④–⑤.

Wachspress[4] attempted to generalize the construction of the shape functions on polygons in a form of rational-fraction. In his approach, the shape functions are called wedges and formed such that the wedge as-

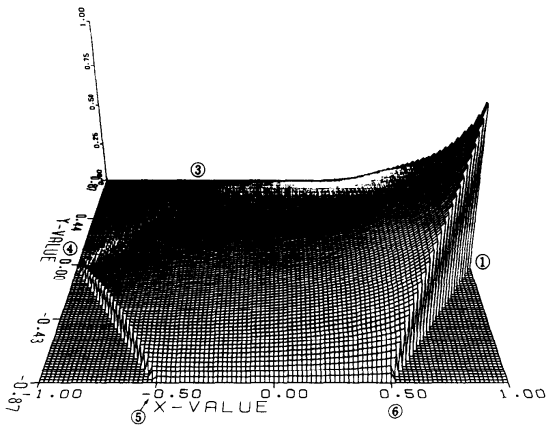

Fig. 8 Hexagonal shape function φ_1 without continuity property.

sociated with vertex k is linear on sides adjacent to k. This linearity is achieved by putting the external diagonal equations of the polygon into the denominator of the wedges, and provides the inter-element continuity of the basis functions. But unfortunately, a degree one approximation can not be attained for the convex polygons except for quadrilaterals. For the case of regular hexagon, the wedge associated with the vertex 1 is:

$$\varphi_1=(1-2/\sqrt{3}y)(1+x-1/\sqrt{3}y)\times(1+x+1/\sqrt{3}y)(1+2/\sqrt{3}y)/\{9(1-1/3x-1/\sqrt{3}y)(1-1/3x+1/\sqrt{3}y)\}. \quad (4.8)$$

In the above, linearity on the adjacent sides ①–② and ①–⑥ can be easily certified. But the function is not a degree one approximation.

5. Numerical Results and Conclusions

It is known[4] that the approximation computed from degree one basis functions differs from the true value by the second order of h (side length) in diffusion equations. The approximation gives the same order of h as the finite difference one. But, it is too sophisticated to evaluate the generic constant for such a tricky scheme as FEM6. Accordingly, we validate the scheme by a comparison with the more refined schemes and also with the analytical solutions of similar geometry. Here we used a set of piecewise rational fraction-type basis functions formed from the shapes (3.5) for FEM6 scheme.

A model problem presented here is the neutron diffusion equation:

$$-D\nabla^2u(X)+\sigma_Au(X)=\lambda(\nu\sigma_F)u(X) \quad X\in V \quad (5.1)$$

where D, σ_A, σ_F, and ν are diffusion coefficient, macroscopic absorption, fission cross section, and the number of neutrons produced by fission, respectively. The equation is solved for neutron flux $u(X)$ for a spatial variable X and the effective multiplication factor λ. The global

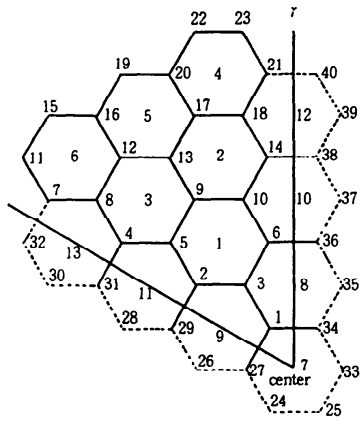

(60°– rotation)

Fig. 9 Critical reactor section of hexagonal geometry (60°-rotational symmetry).

equilibrium equations are treated as an eigenvalue problem and solved by inner and outer double loop iteration method.

The problem taken up here is the case of a one-energy group, homogeneous-region critical reactor of hexagonal prism geometry. The x-y section is shown in Fig. 9 and z-direction is partitioned into the 10 identical size meshes. Here,

H (height) $=100$, $h=11.55$,

$D=3.0$, $\nu\sigma_F=0.021$, $\sigma_A=0.015$, $\sigma_F=0.1$.

We now consider the cylindrical geometry with similar size. From the consideration of the jagged boundary in Fig. 9, we assume that

R (radius) $=75.075$.

The analytical solution is known[7] as

$$u(r,z)=J_0(j_{0,1}/R)\cos(\pi z/H)$$
$$\lambda=\nu\sigma_F(DB^2+\sigma_A)$$

where

$$B^2=(j_{0,1}/R)^2+(\pi/H)^2. \quad (5.2)$$

In the above, J_0 is a Bessel function and $j_{0,1}(=2.405)$ is the smallest positive root of the Bessel function J_0.

The numerical calculations were made on the three different schemes given in Fig. 2. The results are summarized in Table 2. Here the neutron fluxes are normalized by power[2] and the radial fluxes at midplane are shown. The analytical solution in the above sense is shown together. It is seen that the solutions obtained by the three schemes agree with each other and have good accuracy. The difference found between the numerical solutions and the analytical one resulted mostly from the difference of the boundary geometries.

The real scale neutron diffusion problem for the configuration given in Fig. 1 was also calculated. The results obtained from a comparison made between FEM7 and finite difference methods were discussed in Ref. (8). The scheme FEM6 led to a reasonable solution

Table 2 Computed results for three different schemes.

	Power normalized flux			FEM19*	Analytical solution
	FEM6	FEM7	FEM19		
φ_0	—	2.5576	2.4467	1.0	1.0
φ_1	2.4489	2.4552	2.3627	0.96567	0.96607
φ_3	2.1989	2.2015	2.1258	0.86884	0.86771
φ_9	1.3323	1.3172	1.2995	0.53112	0.52296
φ_{13}	0.8156	0.7979	0.8010	0.32736	0.31090
φ_{19}	0.0	0.0	0.0	0.0	0.0
λ	0.99360	0.99193	0.99847	0.99847	1.04028
CPU time on M380	1.11 sec.	2.32 sec.	7.26 sec.		

*normalized by the central flux

with the merit of saving time, where the computing time was reduced to half as compared with the finite difference of triangular meshes. But, the resulting multiplication factor (eigenvalue) differed by 1% and flux (eigenvector) by 9%. Moreover, if the unnormalized shapes in Eq. (3.3) was applied, the eigenvector did not converged within a reasonable time. The use of Eq. (4.7) type shapes resulted in a little more time consuming calculation. The eigenvalue and the eigenvector, however, agree with those by Eq. (3.5) within a tolerable error.

Though the FEM6 scheme does not present decisive advantages for the real scale problem taken up in Fig. 1, the scheme is worth attempting for other problems.

The construction method for shape functions presented here can be applicable for other similar problems based on the hexagon, including irregular ones, as long as identical hexagons are used. If different ones are applied, however, certification of the required order of continuity of basis functions is crucial.

Acknowledgement

The author is very grateful to Dr. Y. Nakahara and Mr. T. Fujimura at Japan Atomic Energy Research Institute (JAERI) for their fruitful discussions. Thanks are also given to Mr. K. Higuchi at JAERI who makes the graphs of shape functions and to Mr. M. Tabei at Tokyo Institute of Technology for the work of Romberg integration.

References

1. HOTTA, M. et al. Applicability of Three Dimensional Diffusion Theory Programs Based on Coarse Mesh Method to Calculating Nuclear Characteristics of Fast Breeder Reactors, *JAERI-M* 9638 (1981).
2. ISE, T. et al. A Computer Problem for Solving Three-Dimensional Neutron Diffusion Equation by the Finite Element Method, *JAERI* 1256 (1978).
3. CONNER, J. J. et al. Finite Element Method For Fluid Flow, Butterworth & Co. Ltd. (1976).
4. WACHSPRESS, E. L. A Rational Finite Element Basis, Academic Press (1975).
5. PRENTER, P. M. Splines and Variational Methods, Jhon Wiley & Sons (1975).
6. HEARN, C. REDUCE2, UCP-19, University of Utah (1973).
7. GREENSPAN, H. et al. Computer Method in Reactor Physics, Gordon and Breach Science Publisher (1968).
8. ISHIGURO, M. and HIGUCHI, K. Application of a Hexagonal Element Scheme in the Finite Element Method to the Three-Dimensional Diffusion Problem of Fast Reactors, *J. Nucl. Sci. and Tech.*, Vol. 20, No. 11 (1983).

(Received June 3, 1983; revised December 16, 1983)